Langmuir

Article

pubs.acs.org/Langmuir

Statistical Analysis of Molecular Nanotemplate Driven DNA Adsorption on Graphite

E. V. Dubrovin,*[,†] S. Speller,[‡] and I. V. Yaminsky[†]

[†]Chair of Physics of Polymers and Crystals, Faculty of Physics, M. V. Lomonosov Moscow State University, Leninskie gory, 1/2, Moscow 119991, Russia

[‡]Institute of Physics, University of Rostock, 18051 Rostock, Germany

Supporting Information

ABSTRACT: In this work, we have studied the conformation of DNA molecules aligned on the nanotemplates of octadecylamine, stearyl alcohol, and stearic acid on highly oriented pyrolytic graphite (HOPG). For this purpose, fluctuations of contours of adsorbed biopolymers obtained from atomic force microscopy (AFM) images were analyzed using the wormlike chain model. Moreover, the conformations of adsorbed biopolymer molecules were characterized by the analysis of the scaling exponent ν, which relates the mean squared end-to-end distance and contour length of the polymer. During adsorption on octadecylamine and stearyl alcohol nanotemplates, DNA forms straight segments, which order along crystallographic axes of graphite. In this case, the conformation of DNA molecules can be described using two different length scales. On a large length scale (at contour lengths $l > 200-400$ nm), aligned DNA molecules have either 2D compact globule or partially relaxed 2D conformation, whereas on a short length scale (at $l \leq 200-400$ nm) their conformation is close to that of rigid rods. The latter type of conformation can be also assigned to DNA adsorbed on a stearic acid nanotemplate. The different conformation of DNA molecules observed on the studied monolayers is connected with the different DNA−nanotemplate interactions associated with the nature of the functional group of the alkane derivative in the nanotemplate (amine, alcohol, or acid). The persistence length of λ-DNA adsorbed on octadecylamine nanotemplates is 31 ± 2 nm indicating the loss of DNA rigidity in comparison with its native state. Similar values of the persistence length (34 ± 2 nm) obtained for 24-times shorter DNA molecules adsorbed on an octadecylamine nanotemplate demonstrate that this rigidity change does not depend on biopolymer length. Possible reasons for the reduction of DNA persistence length are discussed in view of the internal DNA structure and DNA−surface interaction.

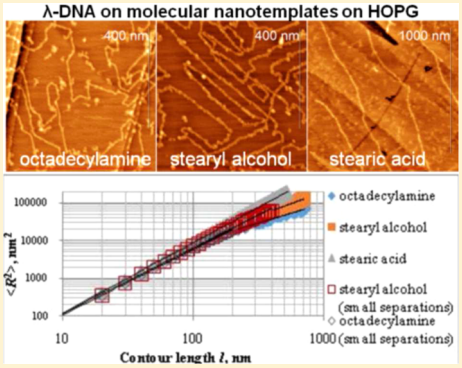

INTRODUCTION

Considerable progress has been made in the understanding of the basic principles of the self-assembly of different organic molecules into monolayers (molecular nanotemplates) on crystal surfaces such as highly oriented pyrolytic graphite (HOPG). The orientation of long chain alkanes and their derivatives (acids, alcohols, amines, etc.) including the precise arrangement of their atoms on the basal plane of graphite has been studied and evaluated both theoretically and experimentally in numerous works (e.g., see refs 1−10). Despite the fact that the first model of alkane chain orientation on graphite appeared long before the invention of scanning probe microscopy (SPM),[11] nowadays, SPM, primarily scanning tunneling microscopy (STM) and atomic force microscopy (AFM), is the main experimental approach for the investigation of self-assembled monolayers because high-resolution images of molecular nanotemplates can be acquired.

Interactions underlying such molecular self-assembly have been analyzed and attributed mainly to van der Waals forces and hydrogen bonding between functional groups of the molecule.[2,6,12,13] The effect of interdigitation of alkyl chains was shown to favor the adsorption of organic molecules on HOPG.[4,14] Moreover, surface properties of molecular nanotemplates can be finely tuned by rational molecule design.[15−17]

The possibility of self-assembly induced unique periodicities of the surface properties of molecular nanotemplates such as morphology, charge, hydrophobicity, roughness, density of hydrogen bonds, as well as the ability of their rational tuning make these monolayers appealing for multiple applications.[18,19] Here, we will focus on the utilization of self-assembled monolayers as substrates for the modification of DNA immobilization. DNA is one of the most important molecules for use in bionanotechnology since it has particular recognition capabilities, high mechanical rigidity, physicochemical stability, and the possibility for repeated denaturation−hybridization cycles.

Indeed, self-assembled monolayers on HOPG have been utilized as substrates for adsorption of polymer molecules,[20]

Received: April 25, 2014
Revised: November 29, 2014
Published: December 3, 2014

ACS Publications © 2014 American Chemical Society

including DNA.[21−24] AFM analysis of DNA molecules immobilized onto the dodecylamine[21−23] and octadecylamine[23,24] nanotemplates revealed stretched biopolymer geometries consisting of straight segments with sharp turns at angles 120° and 60°, reflecting the symmetry of the underlying pattern. This result is an important step toward controlled DNA immobilization on solid substrates in a "bottom-up" approach, a challenging task in bionanotechnology. Such DNA architectures are essential for biosensors and molecular electronic devices; moreover, directed DNA adsorption onto solid conductive substrates may be used for DNA mapping, precise measurements of conductive and mechanical properties of single DNA molecules.[25,26] Graphite is a very appropriate surface for electrochemical studies, such as biosensor applications, due to its low cost, wide potential window, relatively inert electrochemistry, and electrocatalytic activity for a variety of redox reactions.[27−30] It is thought that the development of DNA immobilization methodologies that strongly stabilize DNA on the electrode surface is one of the key factors in DNA biosensor design.[27] At the same time, the degree of surface coverage directly influences the sensor response and can be regarded as the critical issue in the development of a DNA electrochemical biosensor for rapid detection of DNA interaction and damage by hazardous compounds.[27] Therefore, understanding the mechanisms of DNA adsorption on modified graphite surfaces is of great practical importance.

Analysis of AFM images of adsorbed polymers allows one to reveal processes of adsorption and as a consequence information on the interaction with the substrate. Two different scenarios of adsorption of polymers onto molecular nanotemplates have been discussed in previous works:[20,24] they both can be characterized by two different length scales. On a scale of a whole molecule, the conformation in the adsorbed state can be either fully equilibrated or kinetically trapped due to the surface, whereas on a short length scale, the conformation is defined by the molecular nanotemplate. A statistical analysis would be to understand the driving forces for deviating adsorption geometries. To the best of our knowledge, such a statistical analysis of polymer conformations has not been performed for such systems.

Conventional approaches of quantitative description of macromolecular conformation from microscopy images have been recently reviewed by Gallyamov.[31] The procedure most often used for defining the conformation and the persistence length of the macromolecule was first described by Frontali et al.[32] It is based on the wormlike chain model, which requires Gaussian distribution for the angle θ between two tangents to the polymer contour separated by a contour length l:

$$N(\theta(l))_{2D} = (P/2\pi l)^{0.5}\exp(-P\theta^2/2l) \quad (1)$$

where P denotes the persistence length of the macromolecule.

Another approach implies the calculation of the scaling exponent ν, which relates mean squared end-to-end distance and contour length of the polymer l:[33]

$$\langle R^2\rangle = \text{const} \times l^{2\nu} \quad (2)$$

The purpose of this study was to characterize DNA conformation on different molecular nanotemplates on HOPG surfaces from the statistical analysis point of view and to demonstrate the impact of functional groups of the underlying molecular template on the persistence length of adsorbed DNA molecules. The understanding of the DNA conformation on molecular nanotemplates is of utmost importance since it reflects the interaction of a biopolymer with the template and yields information on the adsorption scenario. The persistence length is the fundamental characteristic of a polymer and can be regarded as a measure of the flexibility of the macromolecule. Its variations may indicate important changes of the inner state of DNA molecules, connected with partial denaturation,[34] specific interactions,[35] hydration changes,[36] etc.

In this work, we compare adsorption regimes of DNA on different types of molecular nanotemplates on HOPG. For this reason, we used three derivatives of octadecane: stearic acid ($CH_3(CH_2)_{16}COOH$), octadecylamine ($CH_3(CH_2)_{16}CH_2NH_2$), and stearyl alcohol ($CH_3(CH_2)_{16}CH_2OH$). DNA molecules adsorbed on these nanotemplates were examined with AFM. Conformation of gene molecules was evaluated using statistical analysis of DNA contours according to the above-mentioned approaches. We have also defined the persistence lengths of biomacromolecules adsorbed on the octadecylamine nanotemplate, which appeared to be smaller than that of a native DNA. The decrease of DNA persistence length is discussed with regard to the internal DNA structure and DNA−surface interaction.

MATERIALS AND METHODS

Octadecylamine, stearyl alcohol, and stearic acid were purchased from Sigma-Aldrich and diluted in high purity grade isopropanol (Labtech, Russia) to a final concentration of 5−10 μg/mL (for octadecylamine and stearyl alcohol) and 50 μg/mL (for stearic acid). A 5 μL droplet of obtained solution was deposited onto a rotating freshly cleaved surface of HOPG with a mosaic spread of 0.8° (Atomgraph-crystal, Russia). λ-DNA purchased from Fermentas (in one experiment plasmid linearized 2000 b.p. dsDNA) was diluted in milli-Q water to a final concentration of 0.1 μg/mL. A 20−30 μL portion of λ-DNA solution was deposited on modified HOPG surfaces and after 5 min removed by a flow of clean air.

All experiments were carried out using a multimode atomic force microscope Nanoscope IIIa (Digital Instruments, USA) in tapping mode in air. Commercial polysilicon cantilevers HA_NC (NT-MDT, Russia) with a monocrystal silicon tip exhibiting a curvature radius of about 10 nm were used. Image processing was performed using the FemtoScan software (Advanced Technologies Center, Russia). The scan rate was typically 2 Hz with 512 lines per image.

Contours of DNA molecules (usually within AFM image accessible fractions of them) were traced using a tool "selection of a lengthy object" implemented in the FemtoScan software. Calculation of angle θ as a function of contour length l was performed in Scilab 5.3.3 using an approach described by Frontali et al.[32] The total traced contour length constituted about 100 μm for λ-DNA adsorbed on octadecylamine and stearyl alcohol nanotemplates, 360 μm for 2000 b.p. DNA adsorbed on an octadecylamine nanotemplate, and 180 μm for λ-DNA adsorbed on a stearic acid nanotemplate. Values of θ^2, θ^4, θ^6, and R^2 were averaged for different separations l with an increment size of 10 nm. Since the statistics decreases with the increase of l, for further analysis we considered the values averaged over at least 100 numbers. This condition has cut the l range at 800, 700, and 1400 nm for λ-DNA adsorbed on octadecylamine, stearyl alcohol, and stearic acid nanotemplates correspondingly (and at 500 nm for 2000 b.p. DNA adsorbed on an octadecylamine nanotemplate).

RESULTS AND DISCUSSIONS

Molecular nanotemplates of stearyl alcohol, octadecylamine, and stearic acid on HOPG were prepared by spin coating from their isopropanol solutions. After this, a droplet of DNA solution in water was applied to the surface, left in contact for 5

dx.doi.org/10.1021/la5041773 | Langmuir 2014, 30, 15423−15432

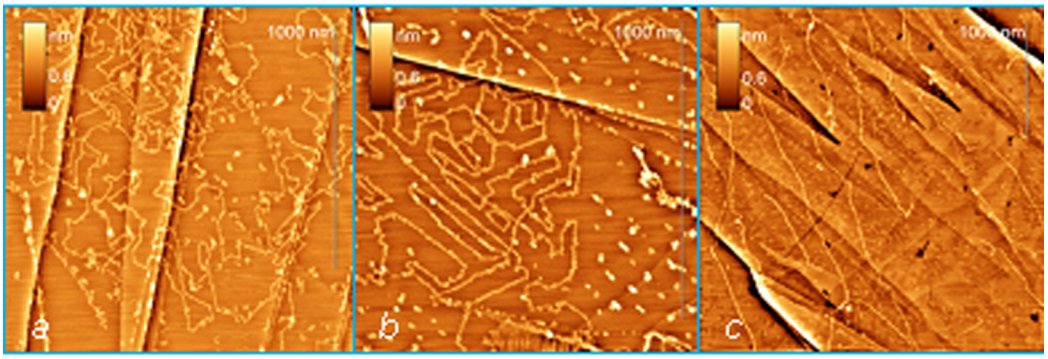

Figure 1. Typical AFM height images of λ-DNA molecules adsorbed on (a) octadecylamine, (b) stearyl alcohol, and (c) stearic acid nanotemplates on HOPG.

min, and blown off with air. The main reason for dilution of DNA in water was to study the impact of the modified surfaces themselves on the DNA adsorption without any additional factors, such as high ionic concentrations, which could influence the adsorption of DNA differently for each surface. Dilute aqueous solutions were also used in the previous works devoted to DNA adsorption on modified graphite,[21−24] but a study from the statistical point of view has not been reported for such systems. The conventional procedure of DNA immobilization on mica also utilizes DNA buffers with very low ionic concentration[37] that makes it possible to compare our results (in particular, the persistence length) with those obtained earlier for DNA adsorbed on mica.

AFM images of λ-DNA adsorbed onto an octadecylamine molecular nanotemplate on HOPG reveal a segmented shape of biopolymers with three-fold symmetry of segment orientation (Figure 1a). This result is in good compliance with earlier observations for DNA self-ordered on octadecylamine and dodecylamine nanotemplates.[22,24] λ-DNA adsorbs on the stearyl alcohol molecular nanotemplate also as a stretched molecule with linear segments oriented along the preferred directions (Figure 1b). It should be noted that self-crossings of DNA contours are either absent or quite rare on AFM images of DNA immobilized on both surfaces.

A different picture of immobilized DNA molecules was observed on a stearic acid nanotemplate (Figure 1c). Though adsorbed DNA molecules in this case are also stretched and do not contain self-crossings, they are all aligned mostly in one direction within one AFM image. Unidirectional alignment of DNA molecules on solid substrates was investigated in different studies[38−41] and was most often attributed to the so-called molecular combing of DNA. The apparent AFM heights and widths (fwhm) of DNA on three studied surfaces are summarized in Table 1. These values are in general agreement with previous results of AFM studies of DNA adsorbed on modified HOPG surfaces.[24,42,43] Here, we should stress the role of the molecular nanotemplates in adsorption of DNA molecules in an expanded form since free adsorption of DNA onto unmodified HOPG results in the formation of molecular networks rather than aligned single molecules[44−46] (see Supporting Information, Figure S1).

Table 1. Mean Values and Their Standard Deviations of AFM Apparent Heights and Widths (fwhm) of DNA Molecules Adsorbed on Molecular Nanotemplates on HOPG

nanotemplate type	height (nm)	width (fwhm) (nm)
stearyl alcohol	1.2 ± 0.2	14 ± 3
stearic acid	0.8 ± 0.2	16 ± 3
octadecylamine	1.1 ± 0.2	9 ± 3

To determine the persistence length of DNA in our experiments, we have applied the approach based on the wormlike chain model.[32] From the distribution function (eq 1), it follows that all odd moments of θ are zero, whereas the first even moments comply with the following relationships:

$$\langle\theta^2(l)\rangle_{2D} = l/P \tag{3}$$

$$\langle\theta^4(l)\rangle_{2D}/\langle\theta^2(l)\rangle^2_{2D} = 3 \tag{4}$$

$$\langle\theta^6(l)\rangle_{2D}/\langle\theta^2(l)\rangle^3_{2D} = 15 \tag{5}$$

Therefore, the persistence length can be determined from the inverse slope of the linear approximation of the observed dependence $\langle\theta^2(l)\rangle_{2D} = f(l)$. For the justification of the applicability of the wormlike chain model to our systems, we first have checked the satisfaction of the relationships 4 and 5, which are the necessary conditions of the Gaussian distribution of θ (eq 1). This test is often used as a criterion of applicability of the wormlike chain model.[32,47]

For analysis of DNA conformation on molecular nanopatterns, the contours of the adsorbed biopolymers were traced using image processing software. Since the surface covered by a whole λ-DNA molecule adsorbed in an extended fashion usually exceeds the size of AFM frames typically used in this study (2−5 μm), our analysis was based on fractions of DNA reachable within one AFM image. For the wormlike chain model, the consideration of DNA fractions instead of the whole molecules should not alter the resulting distribution because contours fluctuate independently according to this model (eq 1).

The calculated values of the ratios from the left side of relationships 4 and 5 for all three types of nanotemplates are presented in Figure 2 along with the theoretical values for the Gaussian distribution function (dotted lines). Large deviations of experimental values are observed for short separations l ($l \leq$ ~50 nm). The rational interpretation is based on the finite pixel size of the images,[47] and we will not consider this region for further analysis.

The moments ratios in (eqs 4−5) for DNA adsorbed on the stearic acid nanotemplate (Figure 2c) are far from their Gaussian values practically for any separations. Such a result is quite as expected for unidirectional contours of adsorbed polymer molecules since the unidirectional shape implies the

dx.doi.org/10.1021/la5041773 | Langmuir 2014, 30, 15423−15432

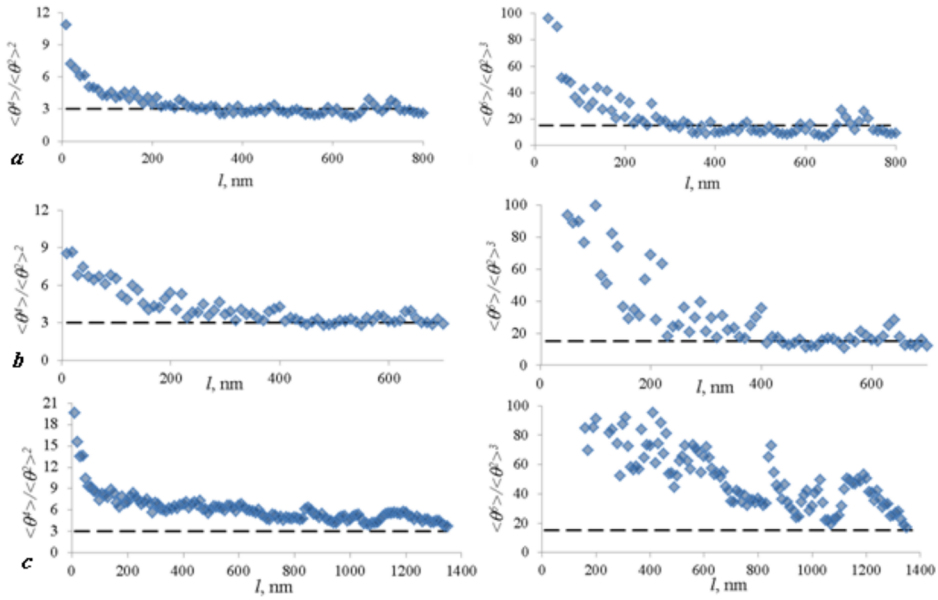

Figure 2. Calculated ratios $\langle\theta^4(l)\rangle/\langle\theta^2(l)\rangle^2$ (left) and $\langle\theta^6(l)\rangle/\langle\theta^2(l)\rangle^3$ (right) for λ-DNA adsorbed on (a) octadecylamine, (b) stearyl alcohol, and (c) stearic acid nanotemplates on HOPG.

presence of some strong force acting on DNA upon its adsorption that prevents the equilibrium of this process. In fact, a nanotemplate of stearic acid can create the conditions (e.g., weak DNA−surface interaction) favoring the molecular combing of DNA, which is caused by the movement of the DNA containing droplet upon its removal from the surface. Such a mechanism was described in different studies of molecular combing.[39,41,48] It was demonstrated that surface tension forces of the receding meniscus far exceed the hydrodynamic forces connected with the movement of the droplet.[48] Therefore, surface tension is a real driving force of molecular combing, which results in aligning of DNA molecules along the normal direction of the receding meniscus. It should be noted that another mechanism of molecular combing of DNA, by gas flow, has also been reported.[40]

In contrast, for DNA molecules adsorbed on octadecylamine and stearyl alcohol nanotemplates there is a range of separations l, at which the ratios $\langle\theta^4(l)\rangle_{2D}/\langle\theta^2(l)\rangle^2_{2D}$ and $\langle\theta^6(l)\rangle_{2D}/\langle\theta^2(l)\rangle^3_{2D}$ are quite close to their Gaussian values (Figure 2a,b). These ratios adopt Gaussian values roughly beyond lengths of ∼200 and ∼400 nm for DNA, adsorbed on octadecylamine and stearyl alcohol nanotemplates, respectively. The observed behavior of the moments ratios indicates that DNA adsorption on these nanotemplates may be considered on two different length scales, short and large, which are characterized by non-Gaussian and Gaussian values of moments ratios of θ.

Non-Gaussian behavior of θ-distributions on a short length scale should be a consequence of the linear segmented shape of the adsorbed DNA molecules. In fact, all mutual angles between tangents to the biopolymer contour inside one segment will be zero, whereas inside two adjacent segments − ±120° or ±60°. Since the real segments are not ideally straight, in practice angles θ will deviate from these values and vary around them. Thus, the distribution of angles θ for small l, not exceeding the length of two adjacent segments, will have well-pronounced maximums and therefore substantially differ from the Gaussian distribution.

If we continue considering adjacent sections of biopolymer contours (i.e., increasing l), new peaks originating by 60° changes will appear in the distribution. Nonideal three-fold symmetry of the directions of DNA segments (e.g., the presence of some portion of other angles between the segments), a finite curvature radius of bends of biopolymer contours, and the earlier mentioned imperfect linearity of DNA segments lead to a significant smearing of the peaks on the distribution and making it approach its shape Gaussian. This is indicated by the analyzed ratios of the even moments of θ upon further increase of separations l (Figure 2a,b). Nevertheless, even on a large statistical sample of angles, these local peaks are often distinguishable on the distributions of θ. As an example, below we perform the analysis of a typical distribution of θ for the separation l demonstrating close to Gaussian values of the moments ratios (eqs 4 and 5).

Two superimposed representations of normalized distribution histograms of θ for l = 320 nm ($\langle\theta^4(l)\rangle_{2D}/\langle\theta^2(l)\rangle^2_{2D}$ = 2.9; $\langle\theta^6(l)\rangle_{2D}/\langle\theta^2(l)\rangle^3_{2D}$ = 13.3), differing by a subdivision of θ, are shown in Figure 3. The filled histogram has the smaller θ-subinterval ($\Delta\theta$ = 0.5 rad or ∼30°) and allows one to resolve some fine structures in the angle θ distribution (in the presented example, these peaks fall approximately on the values ±60°, ±140°, ±230°, etc., which probably reflect values that are multiples of 60°). However, on a coarsened histogram, where the subinterval of θ is larger ($\Delta\theta$ = 1.5 rad or ∼90°, unshaded histogram in Figure 3), this structure disappears due to the compensation of local peaks with nearby minimums. Such a coarsened histogram is well approximated by the Gaussian distribution (the curve in Figure 3). Consequently, the ensemble of real DNA molecules, demonstrating close to theoretical ratios (eqs 4−5) on a large scale, may be associated with the ensemble of ideal Gaussian fashion adsorbed molecules, having the similar coarsened distributions of θ. This is the argument for the justification of using of the wormlike chain model for the coarsened DNA molecules. We should stress that any coarsening of the histograms does not change the calculated values of $\langle\theta^2\rangle$ and other moments of θ because they are based on a fixed statistical sample of angles.

dx.doi.org/10.1021/la5041773 | *Langmuir* 2014, 30, 15423−15432

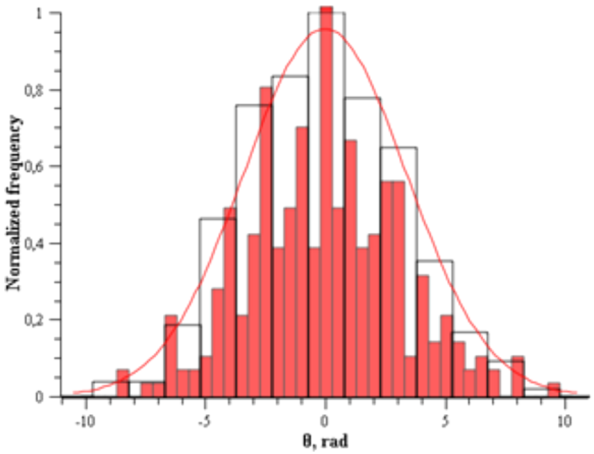

Figure 3. Two superimposed representations of normalized distribution histograms of θ for l = 320 nm (λ-DNA adsorbed on the octadecylamine nanotemplate on HOPG), differing by a subdivision of θ (filled histogram, $\Delta\theta$ = 0.5 rad; unshaded histogram, $\Delta\theta$ = 1.5 rad). The curve denotes the Gaussian approximation of the unshaded histogram.

For the further interpretation of the observed DNA conformations, we have performed the analysis of the scaling exponent ν, which relates mean squared end-to-end distance and contour length of a polymer in accordance with eq 2. For this purpose, we have calculated ν from the slope of the linear regression of the observed dependence $\ln(\langle R^2\rangle) = f(\ln(l))$.

The scaling exponent ν calculated for an ensemble of macromolecules adsorbed on a substrate together with an estimation of a degree of suppression of their self-crossings may serve as criteria for an assignment of macromolecular conformation to a certain type. For instance, rigid rods are characterized by ν = 1, two-dimensional compact globules by ν = 0.5 (without self-crossings), two-dimensional (quasi)-projections of three-dimensional coils by $\nu \approx 0.59$ (self-crossings are allowed), and two-dimensional coils with excluded volume (model of self-assembled walks) by ν = 0.75 (self-crossings are suppressed).[49−51]

We have calculated the scaling exponent ν for DNA adsorbed on octadecylamine and stearyl alcohol nanotemplates on short and large length scales, in accordance with the behavior of moments ratios (Figure 2a,b). The short length scale corresponded to small separations ($l \leq 200$ nm for DNA on octadecylamine and $l \leq 400$ nm for DNA on stearyl alcohol nanotemplates) and non-Gaussian moments ratios of θ, whereas the large length scale included larger separations ($l >$ 200 and 400 nm for DNA adsorbed on octadecylamine and stearyl alcohol nanotemplates correspondingly), at which $\langle\theta^4(l)\rangle_{2D}/\langle\theta^2(l)\rangle^2_{2D}$ and $\langle\theta^6(l)\rangle_{2D}/\langle\theta^2(l)\rangle^3_{2D}$ are close to their Gaussian values (Figure 2a,b). Here, we have considered the calculated moments ratios close to the corresponding Gaussian value if their difference has not exceeded 20% of the latter.

Correlations between mean-square end-to-end distances and contour lengths for λ-DNA adsorbed on all three studied nanotemplates on HOPG together with their linear (in logarithmic scale) approximations are shown in Figure 4. For DNA adsorbed on octadecylamine nanotemplates on HOPG, the scaling exponent ν calculated for large separations is 0.52 ± 0.02. Taking into account the absence (or in some AFM images a low number) of self-crossings of DNA contours in this case (Figure 1b), we can assign DNA conformation on a large length scale to a two-dimensional compact globule conformation (ν = 0.5). This biopolymer conformation is in full agreement with the wormlike chain (persistence) model (which assumes ν = 0.5 for $l \gg P$). In contrast, the scaling exponent for DNA adsorbed on the stearyl alcohol nanotemplate appeared to be 0.64 ± 0.02 for large separations l. Most likely, the conformation of DNA in this case does not belong to any of the "pure" states. However, it can be assigned to a mixed conformation of two-dimensional (quasi)projections of three-dimensional coils ($\nu \approx 0.59$, self-crossings are allowed) and

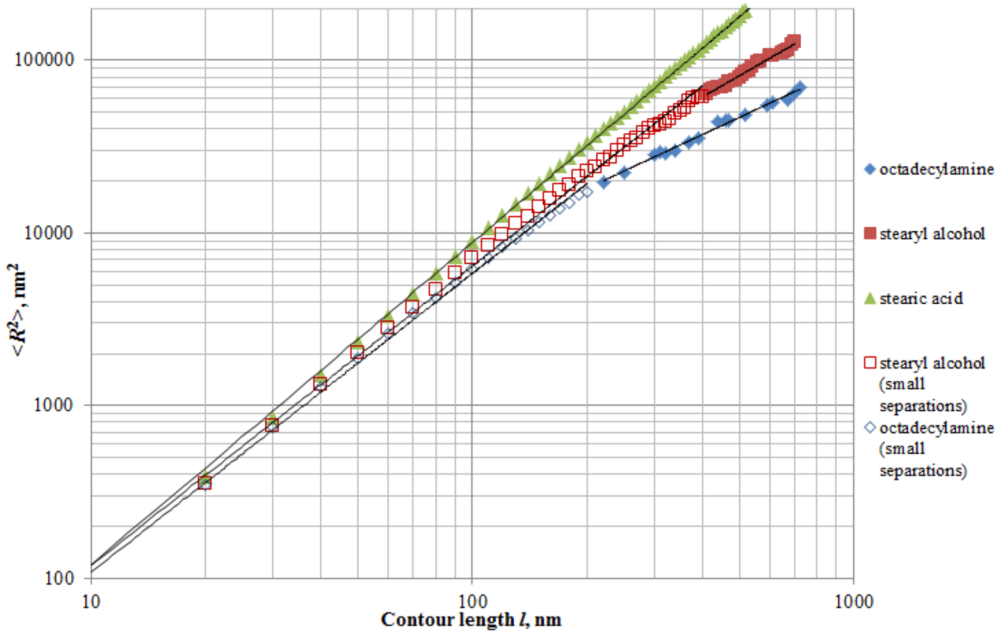

Figure 4. Correlation between mean-square end-to-end distances and contour lengths for λ-DNA molecules adsorbed on octadecylamine, stearyl alcohol, and stearic acid nanotemplates. The lines denote the linear approximations (in logarithmic scale) according to the LS method.

dx.doi.org/10.1021/la5041773 | Langmuir 2014, 30, 15423−15432

two-dimensional coils with excluded volume, described by the model of self-avoiding walk (ν = 0.75, self-crossings are suppressed). Indeed, the presence of a low number of self-crossings of adsorbed DNA molecules (Figure 1c) may indicate only a partial 2D-relaxation of the biopolymer on the surface, which leads to a mixed conformation of DNA on the stearyl alcohol nanotemplate. Similar DNA conformation was observed for weakly adsorbed DNA knots.[52]

At the same time, evaluation of ν for small separations gives the value of 0.87 ± 0.01 for both nanotemplates. This value is quite close to ν = 1 that characterizes the conformation of rigid rods. It is worth noting that this ν value is obtained for separations significantly larger than a persistence length of DNA and, therefore, is not a consequence of the persistence model (which implies $\nu \approx 1$ for $l \leq P$[49]). However, the proximity of the obtained ν value to 1 agrees well with the linear shape of DNA segments, which have almost pure rigid rod conformation.

We should stress that the conformation type of DNA extracted from the ν value on short length scales does not reflect the intrinsic rigidity of a biopolymer due to the significant influence of the local DNA−substrate interaction on the DNA conformation (which leads to a local linear straightening of DNA molecules). Similar interpretation of the derived ν values, that is, 0.93 ± 0.01, may be applied to DNA adsorbed on the stearic acid nanotemplate with the only difference that the type of biopolymer conformation is the same on both length scales. The measured ν values are summarized in Table 2.

Table 2. Mean Values and Their Standard Deviations of the Scaling Exponent ν and the Persistence Length P for λ-DNA Molecules Adsorbed on Molecular Nanotemplates on HOPG

nanotemplate type	ν	P (nm)
octadecylamine	0.52 ± 0.02	31 ± 2
	0.87 ± 0.01 ($l \leq 200$ nm)	34 ± 2 (for 2000 b.p. DNA)
stearyl alcohol	0.66 ± 0.02	N/A
	0.87 ± 0.01 ($l \leq 400$ nm)	
stearic acid	0.93 ± 0.01	N/A

We attribute the differences in the conformation (and ν values) of DNA molecules adsorbed onto octadecylamine and stearyl alcohol nanotemplates to the different interactions of these nanotemplates with DNA molecules. It is worth noting that alkyl derivatives arranged in the nanotemplate on HOPG are likely to retain their normal basic (or acidic) properties. Indeed, nanotemplates consist of sterically unstrained molecules stabilized by hydrogen bonds, which still remain directly accessible to water molecules in aqueous solution (for some configurations of alkane derivatives, the most bulky group may be directed away from the surface[10]), and therefore, there are no reasons for substantial changes of the acidic properties of the organic molecules. A well-known example of another close packed layer of amphiphiles, retaining positive charge of their amine groups, is diethylaminoethyl-cellulose (DEAE-cellulose).[53] Though the structure of DEAE-cellulose aggregates is far from the structure of octadecylamine pattern in our study, this example demonstrates that not experiencing steric strain closed packed amine groups on the surface retain their properties as a base. Retaining the normal charge of the organic molecules in the monolayers on HOPG was directly demonstrated by Kudernac et al. for monolayers consisting of two macrocycles, neutral and positively charged.[54] In this work, the authors have visualized, using STM, iodide counterions on self-assembled organic monolayers (which are "in plane" structures) and directly localized these counterions on the charged macrocycles, whereas no counterions were observed on the neutral macrocycles.

So, the octadecylamine nanotemplate (pK_a ∼10.65) should be (partly) protonated and positively charged (similar conclusion was also made for octadecylamine and dodecylamine nanotemplates on HOPG[21,22]), whereas the stearyl alcohol (pK_a ∼16.8) nanotemplate is almost neutral at neutral pH values of the DNA solution. That is why we assume that DNA interacts with the stearyl alcohol nanotemplate mainly by van der Waals and hydrophobic interactions, whereas in the case of DNA adsorption on the octadecylamine nanotemplate, electrostatic interaction of oppositely charged phosphate groups of DNA and amine groups of the nanotemplate also takes place. Electrostatics was considered as the main driving force for adsorption of negatively charged DNA on dodecylamine modified HOPG[21] and "GM" modified HOPG.[43] Weaker interaction of DNA with the stearyl alcohol nanotemplate directly leads to the higher ν value in comparison with the case of DNA adsorbed onto the octadecylamine nanotemplate. In terms of conformations, this means that weaker DNA interaction with the surface allows the biopolymer to adopt a more relaxed ("extended") conformation, which is closer to the pure 2D relaxed conformation defined by ν = 0.75. At the same time, electrostatic attraction of DNA to the octadecylamine nanotemplate attenuates biopolymer relaxation on the surface and results in a compact globule conformation.

In contrast, the stearic acid nanotemplate (pK_a ∼4.7) has a slight negative charge at neutral pH values that probably complicates DNA adsorption and makes it the weakest among three studied nanotemplates; however, the adsorption is still possible due to the presence of particular sites on DNA molecules capable of binding by van der Waals or hydrophobic interactions. As was mentioned above, weak DNA−surface interaction creates the conditions favoring molecular combing, which finally results in a unidirectional orientation of the adsorbed DNA molecules, which we observe on the stearic acid nanotemplate (Figure 1c). A similar effect of molecular combing of DNA-single walled carbon nanotube hybrids weakly adsorbed onto like-charged silicon wafers coated with an alkyl-silane monolayer was reported in ref 48. The receding meniscus was demonstrated to be the driving force of such a DNA alignment.[39,41,48] In two other cases (octadecylamine and stearyl alcohol nanotemplates on HOPG), adsorbed DNA molecule orientation did not reveal one preferable direction, which is a characteristic feature of molecular combing (except for some special procedures of molecular combing[48]). This suggests that the role of the external force (e.g., surface tension of the receding meniscus) in aligning of DNA molecules on the substrate becomes negligible in comparison with biopolymer−surface interactions.

The analysis of the moments ratios of θ (Figure 2a) and the scaling exponent ν (Table 2) justifies the use of the persistence model for description of DNA molecules adsorbed on octadecylamine nanotemplates on large length scales (for separations l > 200 nm). In spite of the proximity of the moments ratios of θ to the Gaussian values at separations l >

dx.doi.org/10.1021/la5041773 | Langmuir 2014, 30, 15423−15432

400 nm (Figure 2b), the scaling exponent ν = 0.64 characterizing DNA conformation on the stearyl alcohol nanotemplate does not allow one to describe the biopolymer by the persistence model. Therefore, the calculation of the persistence length from eq 3 is only correct for DNA molecules adsorbed on the octadecylamine nanotemplate.

The persistence length of DNA adsorbed on the octadecylamine nanotemplate was estimated as an inverse slope of the linear regression of the observed dependence $\langle\theta^2(l)\rangle_{2D} = f(l)$ at large separations l (Figure 5) and amounts to 31 ± 2 nm

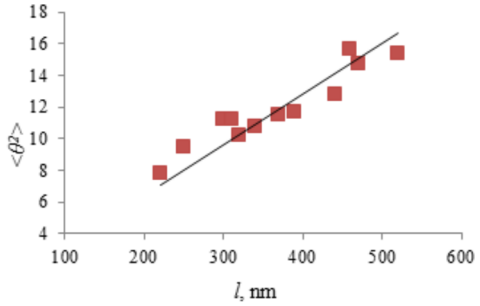

Figure 5. $\langle\theta^2\rangle$ as a function of the segment separation l for λ-DNA adsorbed on the octadecylamine nanotemplate on HOPG. Only l values for which the ratios $\langle\theta^4(l)\rangle_{2D}/\langle\theta^2(l)\rangle^2$ and $\langle\theta^6(l)\rangle_{2D}/\langle\theta^2(l)\rangle^3$ were close to Gaussian values were considered in the evaluation. The line denotes the linear approximations according to the LS method.

(Table 2). It is worth noting that excluded volume effects are negligible for the considered regime of biopolymer lengths (below ~20 persistence lengths) and do not significantly alter the DNA conformation.[47]

To check whether the type of conformation of DNA adsorbed on an octadecylamine nanotemplate on HOPG and its persistence length depend on DNA length, we have made the same adsorption experiment with plasmid linearized 2000 b.p. DNA. AFM images of 2000 b.p. DNA adsorbed on the octadecylamine nanotemplate on HOPG (Figure 6a) resolved similar peculiarities of DNA shape as was observed for λ-DNA (Figure 1a), including the presence of linear segments and a three-fold symmetry of their orientation on the surface. The analysis of the even moments ratios of θ has demonstrated their approach to the Gaussian values for separations l > 250 nm (Figure 6b), which is similar to the behavior of moments ratios of θ for λ-DNA adsorbed on the octadecylamine nanotemplate (Figure 2a). The behavior of the moments ratios of θ allowed in a similar way to separate two length scales and estimate the scaling exponent ν based on the mean end-to-end distance analysis (Figure 6c). The scaling exponent calculated for l > 250 nm is 0.53 ± 0.02, indicating the proximity of the DNA conformation to a of two-dimensional compact globule one. The estimation of the persistence length of 2000 b.p. DNA molecules adsorbed on the octadecylamine nanotemplate gives 34 ± 2 nm (Table 2). Both scaling exponent and persistence length values are in good agreement for the two studied types of DNA molecules adsorbed on octadecylamine nanotemplates on HOPG. This result indicates that biopolymer length does not significantly influence the DNA adsorption scenario and the rigidity of the adsorbed DNA molecules. The independence of the persistence length from the DNA contour length also confirms that excluded volume effects are not significant in the investigated samples.[33]

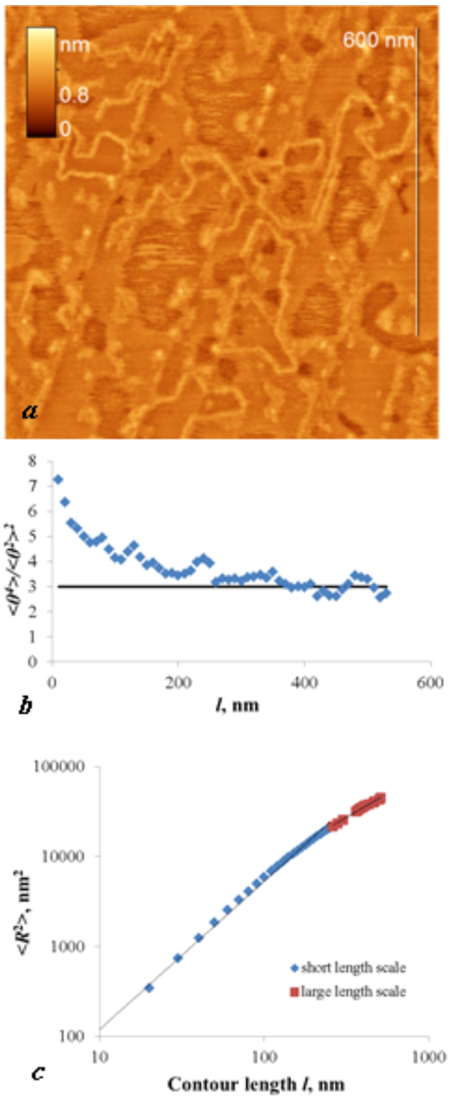

Figure 6. AFM image (a), moments ratio analysis (b), and the mean-square end-to-end distance analysis (c) of 2000 b.p. DNA adsorbed on octadecylamine nanotemplates on HOPG.

The persistence length of DNA adsorbed on mica from weak saline buffers is slightly above 50 nm.[47] Significant reduction of the persistence length and, therefore, rigidity of the DNA molecule adsorbed on the octadecylamine nanopattern may be connected with partial neutralization of the phosphate groups of DNA by positive charges of amine groups of the nanopattern. Podesta et al.[55] have shown that positive surfaces can neutralize up to 50% of phosphate DNA groups and lead up to 5-fold reduction of a persistence length. Moreover, in their experiments upon the reduction of the DNA persistence length to 42 and 37 nm the adsorbed biopolymer conformation complied with the wormlike chain model.

The second reason for the reduction of the rigidity of DNA on the octadecylamine nanopattern may be partial denaturation of adsorbed DNA molecules. Denaturation bubbles were observed on AFM images of DNA adsorbed on octadecylamine[24] and dodecylamine[22] nanopatterns when high-resolution cantilevers (with tip radius about 1 nm) were used. At the same time, authors studying high-resolution AFM imaging of DNA molecules immobilized on mica in a relaxed conformation did not report about any denaturation bubbles

dx.doi.org/10.1021/la5041773 | Langmuir 2014, 30, 15423−15432

(e.g., ref 56). The reason for partial denaturation is probably connected with the linear shape of DNA segments. Indeed, multiple works have demonstrated that denaturation bubbles appear on a straightened DNA molecule (e.g., refs 57 and 58). Formation of denaturation bubbles occurs due to the underwinding of the DNA double helix: denaturation bubbles relieve the twist experienced by the remainder of the double helix, thus making this process energetically favorable.[59] Like the whole stretched biopolymer, its linear segments also experience underwinding of the double helix that may lead to the formation of denaturation bubbles. Hwa et al. supposed that denaturation bubbles, which are formed due to DNA stretching, have longer lifetimes than thermally denatured bubbles since the applied twist plays the role of an energy barrier preventing bubble annihilation.[60] In our system, the interaction between the opened bases of the DNA double helix and the molecular nanopattern (e.g., hydrophobic interaction or formation of hydrogen bonds) may be the additional factor stabilizing denaturation bubbles on the surface.

CONCLUSIONS

We have shown using AFM, that DNA aligns on octadecylamine, stearyl alcohol, and stearic acid nanotemplates on HOPG. Statistical analysis of contour fluctuations and estimation of the scaling exponent ν demonstrate that DNA molecules adsorbed on octadecylamine and stearyl alcohol nanotemplates can be characterized on two length scales. On a short length scale (for separations $l \leq 200-400$ nm), the conformation of adsorbed DNA molecules can be characterized by non-Gaussian fluctuations of their contours and the scaling exponent value of $\nu = 0.87 \pm 0.01$, which is close to the theoretical value of $\nu = 1$, corresponding to the rigid rod conformation of a polymer. This conformation can be explained by the local straitening of DNA molecules by the nanotemplates. In contrast, on a large length scale ($l > 200-400$ nm) DNA contours fluctuate much closer to Gaussian distribution, according to its necessary conditions (eqs 4−5). However, DNA conformations defined from the scaling exponent on a large length scale are different. The conformation of DNA molecules adsorbed on the octadecylamine nanotemplate can be assigned to the compact globule conformation ($\nu = 0.52 \pm 0.02$), which corresponds to the persistence model. At the same time, a mixed conformation can be assigned to biopolymers adsorbed on the stearyl alcohol nanotemplate, which are characterized by $\nu = 0.64 \pm 0.02$. This mixed conformation implies a kinetic trapping of the three-dimensional DNA conformation in solution followed by a partial relaxation of the molecules on the surface. DNA molecules adsorbed on the stearic acid nanotemplate have rigid rod conformation, indicating the influence of some strong force upon biopolymer adsorption or the influence of the air flow in combination with a weak binding to the molecule layer.

We have clearly demonstrated that a change of a single functional group in an organic molecule forming a molecular nanotemplate on HOPG significantly influences the conformation of DNA molecules adsorbed on this nanotemplate. This happens due to the different DNA−nanotemplate interactions associated with the functional group of a HOPG modifier (amine, alcohol, or acid). Moreover, the conformation of the adsorbed biopolymer may be different on different length scales.

DNA molecules self-ordered on molecular nanotemplates on HOPG may still behave as a wormlike chain on a large length scale (as on octadecylamine nanotemplates). This interesting result can be interpreted as self-ordering of DNA around its wormlike chain conformation on the surface. Such interpretation provides a better understanding of reasons underlying the observed DNA configurations on the nanotemplates and allows one to look at the intrinsic property of the biopolymer, such as the persistence length. The persistence length of λ-DNA adsorbed on the octadecylamine nanotemplate turns out to be 31 ± 2 nm. Almost the same value of the persistence length (34 ± 2 nm) has been also determined for shorter DNA molecules adsorbed on an octadecylamine nanotemplate. Partial DNA denaturation may be one of the main reasons for the reduction of the persistence length and, therefore, the rigidity of the adsorbed biopolymer in comparison with the native state of DNA in weak saline solutions. The obtained results also give new insight into possible applications of such biopolymer systems, e.g., for constructing self-assembled DNA architectures with tunable DNA rigidity and level of denaturation.

ASSOCIATED CONTENT

Supporting Information

AFM image of DNA molecules adsorbed on the freshly cleaved HOPG. This material is available free of charge via the Internet at http://pubs.acs.org.

AUTHOR INFORMATION

Corresponding Author

*E-mail: dubrovin@polly.phys.msu.ru.

Notes

The authors declare no competing financial interest.

ACKNOWLEDGMENTS

We thank Dr. M. O. Gallyamov, Dr. O. N. Koroleva, and Dr. V. L. Drutsa for valuable discussions of the manuscript. The President Grant Program for Young Researchers (MK-312.2013.2) is acknowledged.

ABBREVIATIONS

AFM, atomic force microscopy; HOPG, highly oriented pyrolytic graphite

REFERENCES

(1) Rabe, J. P.; Buchholz, S. Commensurability and Mobility in Two-Dimensional Molecular Patterns on Graphite. *Science* **1991**, *253*, 424−427.

(2) Medina, S.; Benítez, J. J.; Castro, M. A.; Cerrillos, C.; Millán, C.; Alba, M. D. Monolayer Arrangement of Fatty Hydroxystearic Acids on Graphite: Influence of Hydroxyl Groups. *Thin Solid Films* **2013**, *539*, 194−200.

(3) Silly, F. Moire Pattern Induced by the Electronic Coupling between 1-Octanol Self-Assembled Monolayers and Graphite Surface. *Nanotechnology* **2012**, *23*, 225603.

(4) Yang, T.; Berber, S.; Liu, J.-F.; Miller, G. P.; Tománek, D. Self-Assembly of Long Chain Alkanes and Their Derivatives on Graphite. *J. Chem. Phys.* **2008**, *128*, 124709.

(5) Krukowski, P.; Klusek, Z.; Olejniczak, W.; Klepaczko, R.; Puchalski, M.; Dabrowski, P.; Kowalczyk, P.J.; Gwozdzinski, K. Self-Assembled Monolayers of Radical Molecules Physisorbed on HOPG(0001) Substrate Studied by Scanning Tunnelling Microscopy and Electron Paramagnetic Resonance Techniques. *Appl. Surf. Sci.* **2009**, *255*, 8769−8773.

(6) Prokhorov, V. V.; Klinov, D. V.; Chinarev, A. A.; Tuzikov, A. B.; Gorokhova, I. V.; Bovin, N. V. High-Resolution Atomic Force

Microscopy Study of Hexaglycylamide Epitaxial Structures on Graphite. *Langmuir* **2011**, *27*, 5879−5890.
(7) Hibino, M.; Sumi, A.; Tsuchiya, H.; Hatta, I. Microscopic Origin of the Odd-Even Effect in Monolayer of Fatty Acids Formed on a Graphite Surface by Scanning Tunneling Microscopy. *J. Phys. Chem. B* **1998**, *102*, 4544−4547.
(8) Ohlendorf, G.; Mahler, C. W.; Jester, S.-S.; Schnakenburg, G.; Grimme, S.; Höger, S. Highly Strained Phenylene Bicyclophanes. *Angew. Chem., Int. Ed.* **2013**, *52*, 12086−12090.
(9) Hiasa, T.; Onishi, H. Competitive Adsorption on Graphite Investigated Using Frequency-Modulation Atomic Force Microscopy: Interfacial Liquid Structure Controlled by the Competition of Adsorbed Species. *Langmuir* **2013**, *29*, 5801−5805.
(10) De Cat, I.; Gobbo, C.; Van Averbeke, B.; Lazzaroni, R.; De Feyter, S.; van Esch, J. Controlling the Position of Functional Groups at the Liquid/Solid Interface: Impact of Molecular Symmetry and Chirality. *J. Am. Chem. Soc.* **2011**, *133*, 20942−20950.
(11) Groszek, A. J. Selective Adsorption at Graphite/Hydrocarbon Interfaces. *Proc. R. Soc. London, Ser. A* **1970**, *314*, 473−498.
(12) Dickerson, N.; Hibberd, A. M.; Oncel, N.; Bernasek, S. L. Hydrogen-Bonding versus van der Waals Interactions in Self-Assembled Monolayers of Substituted Isophthalic Acids. *Langmuir* **2010**, *26*, 18155−18161.
(13) den Boer, D.; Habets, T.; Coenen, M. J. J.; van der Maas, M.; Peters, T. P. J.; Crossley, M. J.; Khoury, T.; Rowan, A. E.; Nolte, R. J. M.; Speller, S.; Elemans, J. A. A. W. Controlled Templating of Porphyrins by a Molecular Command Layer. *Langmuir* **2011**, *27*, 2644−2651.
(14) Arrigoni, C.; Schull, G.; Bléger, D.; Douillard, L.; Fiorini-Debuisschert, C.; Mathevet, F.; Kreher, D.; Attias, A.-J.; Charra, F. J. Structure and Epitaxial Registry on Graphite of a Series of Nanoporous Self-Assembled Molecular Monolayers. *Phys. Chem. Lett.* **2010**, *1*, 190−194.
(15) Tahara, K.; Furukawa, S.; Uji-i, H.; Uchino, T.; Ichikawa, T.; Zhang, J.; Mamdouh, W.; Sonoda, M.; De Schryver, F.C.; De Feyter, S.; Tobe, Y. Two-Dimensional Porous Molecular Networks of Dehydrobenzo[12]annulene Derivatives via Alkyl Chain Interdigitation. *J. Am. Chem. Soc.* **2006**, *128*, 16613−16625.
(16) Miyake, K.; Hori, Y.; Ikeda, T.; Asakawa, M.; Shimizu, T.; Sasaki, S. Alkyl Chain Length Dependence of the Self-Organized Structure of Alkyl-Substituted Phthalocyanines. *Langmuir* **2008**, *24*, 4708−4714.
(17) De Feyter, S.; Gesquire, A.; Klapper, M.; Mllen, K.; De Schryver, F.C. Toward Two-Dimensional Supramolecular Control of Hydrogen-Bonded Arrays: The Case of Isophthalic Acids. *Nano Lett.* **2003**, *3*, 1485−1488.
(18) Tao, F. Nanoscale Surface Chemistry in Self- and Directed-Assembly of Organic Molecules on Solid Surfaces and Synthesis of Nanostructured Organic Architectures. *Pure Appl. Chem.* **2008**, *80*, 45−57.
(19) Claridge, S. A.; Liao, W.-S.; Thomas, J. C.; Zhao, Y.; Cao, H. H.; Cheunkar, S.; Serino, A. C.; Andrews, A. M.; Weiss, P. S. From the Bottom Up: Dimensional Control and Characterization in Molecular Monolayers. *Chem. Soc. Rev.* **2013**, *42*, 2725−2745.
(20) Severin, N.; Okhapkin, I. M.; Khokhlov, A. R.; Rabe, J. P. Adsorption of Polyelectrolyte Molecules to a Nanostructured Monolayer of Amphiphiles. *Nano Lett.* **2006**, *6*, 1018−1022.
(21) Severin, N.; Barner, J.; Kalachev, A. A.; Rabe, J. P. Manipulation and Overstretching of Genes on Solid Substrates. *Nano Lett.* **2004**, *4*, 577−579.
(22) Adamcik, J.; Tobenas, S.; Di Santo, G.; Klinov, D.; Dietler, G. Temperature-Controlled Assembly of High Ordered/Disordered Dodecylamine Layers on HOPG: Consequences for DNA Patterning. *Langmuir* **2009**, *25*, 3159−3162.
(23) Severin, N.; Zhuang, W.; Ecker, C.; Kalachev, A. A.; Sokolov, I. M.; Rabe, J. P. Blowing DNA Bubbles. *Nano Lett.* **2006**, *6*, 2561−2566.
(24) Dubrovin, E. V.; Gerritsen, J. W.; Zivkovic, J.; Yaminsky, I. V.; Speller, S. The Effect of Underlying Octadecylamine Monolayer on the DNA Conformation on the Graphite Surface. *Colloids Surf., B* **2010**, *76*, 63−69.
(25) Bustamante, C.; Smith, S. B.; Liphardt, J.; Smith, D. Single-Molecule Studies of DNA Mechanics. *Curr. Opin. Struct. Biol.* **2000**, *10*, 279−285.
(26) Chepelianskii, A. D.; Klinov, D.; Kasumov, A.; Gueron, S.; Pietrement, O.; Lyonnais, S.; Bouchiat, H. Conduction of DNA Molecules Attached to a Disconnected Array of Metallic Ga Nanoparticles. *New J. Phys.* **2011**, *13*, 063046.
(27) Ensafi, A. A.; Heydari-Bafrooei, E.; Dinari, M.; Mallakpour, S. Improved Immobilization of DNA to Graphite Surfaces, Using Amino Acid Modified Clays. *J. Mater. Chem. B* **2014**, *2*, 3022−3028.
(28) McCreery, R. L. Advanced Carbon Electrode Materials for Molecular Electrochemistry. *Chem. Rev.* **2008**, *108*, 2646−2687.
(29) Walcarius, A. Electrocatalysis, Sensors and Biosensors in Analytical Chemistry Based on Ordered Mesoporous and Macroporous Carbon-Modified Electrodes. *Trends Anal. Chem.* **2012**, *38*, 79−97.
(30) Peng, Z.; Zhang, D.; Shi, L.; Yan, T. High Performance Ordered Mesoporous Carbon/Carbon Nanotube Composite Electrodes for Capacitive Deionization. *J. Mater. Chem.* **2012**, *22*, 6603−6612.
(31) Gallyamov, M. O. Scanning Force Microscopy as Applied to Conformational Studies in Macromolecular Research. *Macromol. Rapid Commun.* **2011**, *32*, 1210−1246.
(32) Frontali, C.; Dore, E.; Ferrauto, A.; Gratton, E. An Absolute Method for the Determination of the Persistence Length of Native DNA from Electron Micrographs. *Biopolymers* **1979**, *18*, 1353−1373.
(33) Stokke, B. T.; Brant, D. A. The Reliability of Wormlike Polysaccharide Chain Dimensions Estimated from Electron Micrographs. *Biopolymers* **1990**, *30*, 1161−1181.
(34) Meyer, S.; Jost, D.; Theodorakopoulos, N.; Peyrard, M.; Lavery, R.; Everaers, R. Temperature Dependence of the DNA Double Helix at the Nanoscale: Structure, Elasticity, and Fluctuations. *Biophys. J.* **2013**, *105*, 1904−1914.
(35) Cesconetto, E. C.; Junior, F. S. A.; Crisafuli, F. A. P.; Mesquita, O. N.; Ramos, E. B.; Rocha, M. S. DNA Interaction with Actinomycin D: Mechanical Measurements Reveal the Details of the Binding Data. *Phys. Chem. Chem. Phys.* **2013**, *15*, 11070−11077.
(36) Hormen, S.; Ibarra, B.; Valpuesta, J. M.; Carrascosa, J. L.; Arias-Gonzalez, J. R. Mechanical Stability of Low-Humidity Single DNA Molecules. *Biopolymers* **2012**, *97*, 199−208.
(37) Lyubchenko, Y. L.; Shlyakhtenko, L. S.; Ando, T. Imaging of Nucleic Acids with Atomic Force Microscopy. *Methods* **2011**, *54*, 274−283.
(38) Dubrovin, E. V.; Staritsyn, S. N.; Yakovenko, S. A.; Yaminsky, I. V. Self-Assembly Effect During the Adsorption of Polynucleotides on Stearic Acid Langmuir-Blodgett Monolayer. *Biomacromolecules* **2007**, *8*, 2258−2261.
(39) Bensimon, A.; Simon, A.; Chiffaudel, A.; Croquette, V.; Heslot, F.; Bensimon, D. Alignment and Sensitive Detection of DNA by a Moving Interface. *Science* **1994**, *265*, 2096−2098.
(40) Li, J.; Bai, C.; Wang, C.; Zhu, C.; Lin, Z.; Li, Q.; Cao, E. A Convenient Method of Aligning Large DNA Molecules on Bare Mica Surfaces for Atomic Force Microscopy. *Nucleic Acids Res.* **1998**, *26*, 4785−4786.
(41) Bensimon, D.; Simon, A.; Croquette, V.; Bensimon, A. Stretching DNA with a Receding Meniscus − Experiments and Models. *Phys. Rev. Lett.* **1995**, *74*, 4754−4757.
(42) Klinov, D. V.; Dubrovin, E. V.; Yaminsky, I. V. Substrate for Scanning Probe Microscopy of DNA: HOPG versus Mica. *Phys. Low-Dimens. Struct.* **2003**, *3*−*4*, 119−124.
(43) Adamcik, J.; Klinov, D. V.; Witz, G.; Sekatskii, S. K.; Dietler, G. Observation of Single-Stranded DNA on Mica and Highly Oriented Pyrolytic Graphite by Atomic Force Microscopy. *FEBS Lett.* **2006**, *580*, 5671−5675.
(44) Brett, A. M. O.; Chiorcea, A. M. Atomic Force Microscopy of DNA Immobilized onto a Highly Oriented Pyrolytic Graphite Electrode Surface. *Langmuir* **2003**, *19*, 3830−3839.

(45) Paquim, A. M. C.; Oretskaya, T. S.; Brett, A. M. O. Adsorption of Synthetic Homo- and Hetero-Oligodeoxynucleotides onto Highly Oriented Pyrolytic Graphite: Atomic Force Microscopy Characterization. *Biophys. Chem.* **2006**, *121*, 131−141.
(46) Jiang, X. H.; Lin, X. Q. Atomic Force Microscopy of DNA Self-Assembled on a Highly Oriented Pyrolytic Graphite Electrode Surface. *Electrochem. Commun.* **2004**, *6*, 873−879.
(47) Rivetti, C.; Guthold, M.; Bustamante, C. Scanning Force Microscopy of DNA Deposited onto Mica: Equilibration versus Kinetic Trapping Studied by Statistical Polymer Chain Analysis. *J. Mol. Biol.* **1996**, *264*, 919−932.
(48) Khripin, C. Y.; Zheng, M.; Jagota, A. Deposition and Meniscus Alignment of DNA−CNT on a Substrate. *J. Colloid Interface Sci.* **2009**, *330*, 255−265.
(49) Joanicot, M.; Revet, B. DNA Conformational Studies from Electron Microscopy. I. Excluded Volume Effect and Structure Dimensionality. *Biopolymers* **1987**, *26*, 315−326.
(50) Maier, B.; Rädler, J. O. Conformation and Self-Diffusion of Single DNA Molecules Confined to Two Dimensions. *Phys. Rev. Lett.* **1999**, *82*, 1911−1914.
(51) Lin, P.-K.; Fu, C.-C.; Chen, Y.-L.; Chen, Y.-R.; Wei, P.-K.; Kuan, C. H.; Fann, W. S. Static Conformation and Dynamics of Single DNA Molecules Confined in Nanoslits. *Phys. Rev. E* **2007**, *76*, 011806.
(52) Ercolini, E.; Valle, F.; Adamcik, J.; Witz, G.; Metzler, R.; Rios, P. D. L.; Roca, J.; Dietler, G. Fractal Dimension and Localization of DNA Knots. *Phys. Rev. Lett.* **2007**, *98*, 058102.
(53) Davila, C.; Charles, P.; Ledoux, L. The Chromatography of Nucleic Acid Preparations on DEAE-Cellulose Paper. I. Fractionation of Deoxyribonucleic Acid on Paper Strips or on Centrifuged Paper Pulp. *J. Chromatogr.* **1965**, *19*, 382−395.
(54) Kudernac, T.; Shabelina, N.; Mamdouh, W.; Höger, S.; De Feyter, S. STM visualisation of counterions and the effect of charges on self-assembled monolayers of macrocycles. *Beilstein J. Nanotechnol.* **2011**, *2*, 674−680.
(55) Podesta, A.; Indrieri, M.; Brogioli, D.; Manning, G. S.; Milani, P.; Guerra, R.; Finzi, L.; Dunlap, D. Positively Charged Surfaces Increase the Flexibility of DNA. *Biophys. J.* **2005**, *89*, 2558−2563.
(56) Klinov, D. V.; Neretina, T. V.; Prokhorov, V. V.; Dobrynina, T. V.; Aldarov, K. G.; Demin, V. V. High-Resolution Atomic Force Microscopy of DNA. *Biochemistry (Moscow)* **2009**, *74*, 1150−1154.
(57) Strick, T. R.; Allemand, J.-F.; Bensimon, D.; Bensimon, A.; Croquette, V. The Elasticity of a Single Supercoiled DNA Molecule. *Science* **1996**, *271*, 1835−1837.
(58) Strick, T. R.; Allemand, J.-F.; Bensimon, D.; Croquette, V. Behavior of Supercoiled DNA. *Biophys. J.* **1998**, *74*, 2016−2028.
(59) Cocco, S.; Monasson, R. Statistical Mechanics of Torque Induced Denaturation of DNA. *Phys. Rev. Lett.* **1999**, *83*, 5178−5181.
(60) Hwa, T.; Marinari, E.; Sneppen, K.; Tang, L.-H. Localization of Denaturation Bubbles in Random DNA Sequences. *Proc. Natl. Acad. Sci. U.S.A.* **2003**, *100*, 4411−4416.